Available online at www.sciencedirect.com
SCIENCE DIRECT®
ELSEVIER
Journal of Nuclear Materials 329–333 (2004) 630–633
journal of nuclear materials
www.elsevier.com/locate/jnucmat

Swelling and post-irradiated deformation structures in 18Cr–10Ni–Ti irradiated with heavy ions

O.V. Borodin *, V.V. Bryk, A.S. Kalchenko, I.M. Neklyudov, A.A. Parkhomenko, V.N. Voyevodin

Institute of Solid State Physics, Materials and Technology NSC KIPT, 1 Akademicheskaya st, 61108 Kharkov, Ukraine

Abstract

The current work presents irradiation microstructure evolution in 18Cr–10Ni–Ti SS after Cr ion irradiation and tensile deformation. TEM and tensile samples were irradiated to a total dose of 1, 5, 10 and 100 dpa with 2 MeV Cr^{3+} ions at 305 °C (8×10^{-4} dpa/s) and 600 °C (10^{-2} dpa), respectively. Damage structure at 305 °C consists of high density of black dots, loops, which are less than 10 nm in diameter (1–5 dpa), at saturation number density 2×10^{22} m^{-3}. Deformation behavior of irradiated steel is manifested as a transition from twinning to dislocation channeling with test temperature and dose increasing. Damage at 635 °C is a different volumes of swelling: ~0.2–0.4% at 5 dpa and ~20% at 100 dpa. Irradiated samples showed a strong role of voids in the matrix and grain boundary fracture processes.

1. Introduction

Austenitic stainless steel are the main structure materials for vacuum vessel and most in-vessel components for ITER [1,2]. The ITER components will operate in the temperature interval 50–300 °C. This regime is below the usual temperature range for significant void swelling, but corresponds to a range of low temperature embrittlement.

Most crucial irradiation/test temperature is the 300 °C, which corresponds to maximum values of the lack of macroscopic ductility [3]. During deformation of irradiated specimens the uniform strain is practically absent and flow localization effects are observed. Operation within the temperature-dose regime where intense flow localization occurs requires modification of engineering design rules to protect the structure against low macroscopic ductility failure.

The radiation damage structures in stainless steel and the relationship between the damage structure and the changes in deformation mode and mechanical behavior are discussed.

2. Experimental

Austenitic stainless steel 18Cr–10Ni–Ti in solution-annealed condition (1050 °C, 30 min) was examined. The chemical composition of this steel is 0.08C, 0.3Si, 1.2 Mn, 18.2Cr, 10.4Ni, 0.2Ti. Ion irradiation was carried out in the ESUVI (Electrostatic Accelerator with External Injector in NSC KIPT (Ukraine) heavy ion accelerator with 2 MeV Cr^{3+} ions at a peak damage rate of 10^{-2} dpa/s at temperature 635 °C (dose of 100 dpa) and damage rate of 8×10^{-4} dpa/s at temperature 305 °C (doses of 1, 5, and 10 dpa).

The irradiated and unirradiated specimens were in the form of flat tensile specimens with an overall length of 50 mm. The gage length of the specimen is 10 mm long by 3 mm width and by 0.3 nm thick. Using an NIKIMP universal testing machine for the tensile testing the specimens were tested at room temperature and 300 °C (in vacuum) with strain rate of 10^{-3} s^{-1}. The total elongation (7%) was calculated from the engineering stress–strain curve.

* Corresponding author. Tel.: +38-0572 35 6584; fax: +38-0572 35 1703.
E-mail address: borodin@kipt.kharkov.ua (O.V. Borodin).

0022-3115/$ - see front matter
doi:10.1016/j.jnucmat.2004.04.101

Beam with diameter of 12 mm bombarded the investigated specimen. Under this ion energy the damaged layer depth was about 900 nm. The inhomogeneous distribution of radiation damage on depth of ions irradiated material requires to remove the quite fine (~200 nm) surface layer and the layer of increased concentration of implanted interstitial atoms.

The TEM specimens were taken from the deformed area of tensile specimens after testing. Electron microscopy observation were performed with JEM 100cx electron microscope.

3. Results and discussion

3.1. Radiation induced microstructures ($T_{irr} = 305$ °C)

Cr^{3+}-ion irradiation has a significant effect on the microstructure of the Cr–18Ni–10Ti SS. Fig. 1 shows TEM micrographs of the 1, 5, and 10 dpa microstructures.

The 1 dpa samples (Fig. 1(a)) shows a uniform distribution of isolated defects. No voids have been found, only small defect clusters 'black spots'. The density of the black spots was $\sim 2\text{–}3 \times 10^{22}$ m^{-3}, and their diameter is less than a 8 nm.

The samples irradiated to 5 dpa (Fig. 1(b)) have a more complex microstructure. The microstructure consists of a mixture of Frank loops, unfaulted loops, tangles of dislocation and a much lower density of black spots. Total dislocation defect density was $1.5\text{–}2.5 \times 10^{22}$ m^{-3}.

The samples irradiated to 10 dpa (Fig. 1(c)) have a irregular network formed from dislocation tangles and lower density of black spots and loops. Total dislocation defect density was $1\text{–}2 \times 10^{22}$ m^{-3}.

Comparison with the studies which have been performed on 300 series stainless steels irradiated at similar condition ($T_{irr} = 288$ °C, 5 MeV Cr^{2+} ions, doses up to 10 dpa) shows similar parameters of radiation defect structure: black spots saturation level about 3×10^{22} m^{-3} and average loop diameter 15 nm [4].

3.2. Deformation in ion-irradiated 18Cr–10Ni–Ti SS

3.2.1. Room deformation temperature

Twinning is the dominant deformation mechanism in both unirradiated and irradiated (305 °C, 1 dpa) specimens under tensile deformation on. 7% (Fig. 2(a)). Irradiated under the dose of 5 dpa deformed specimens shown the development of substructures with extended dislocation and deformation stacking faults.

3.2.2. Deformation temperature of 300 °C

At the doses of 5 and 10 dpa the plastic flow localization has an appreciable impact on the plastic deformation of the irradiated material and is observed in high quantity. The plastic deformation localization was observed as narrow (≈50–60 nm) shearing bands without the dislocation loops – the so called effect of 'dislocation channeling' coupled with the annihilation of the dislocation loop fraction by dislocations moving into the 'channel' (Fig. 2(b)). At the same time, the larger part of the material volume is undeformed. In comparison with

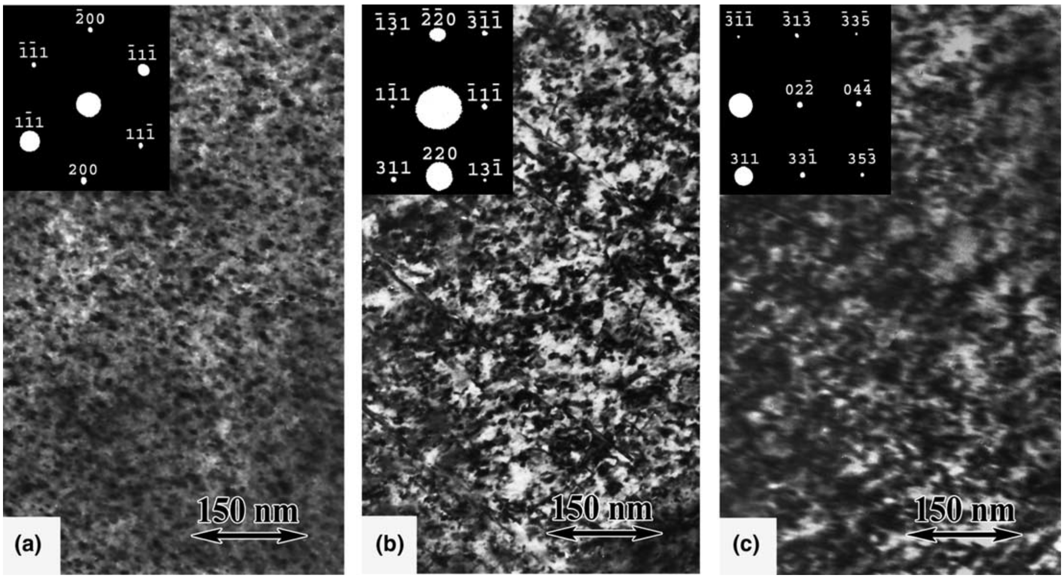

Fig. 1. TEM micrographs of 18Cr–10Ni–Ti SS: (a) irradiated to 1 dpa, (b) irradiated to 5 dpa and (c) irradiated to 10 dpa microstructures ($T_{irr} = 302$ °C).

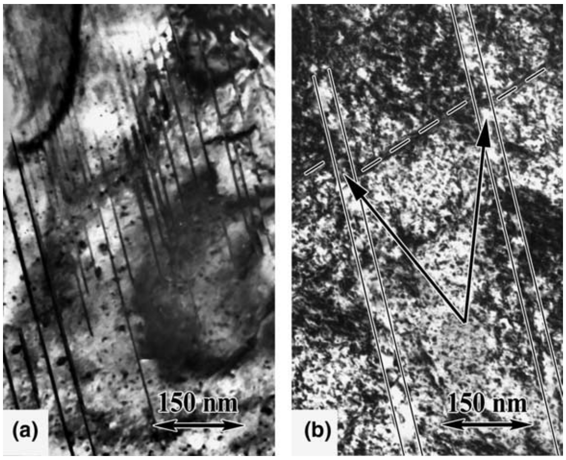

Fig. 2. Microstructures of deformed 18Cr–10Ni–Ti SS samples (7%): (a) irradiated to 1 dpa at 20 °C, and (b) irradiated to 5 dpa and deformed at 300 °C (arrows indicate the sites of channels and deformation twins intersection).

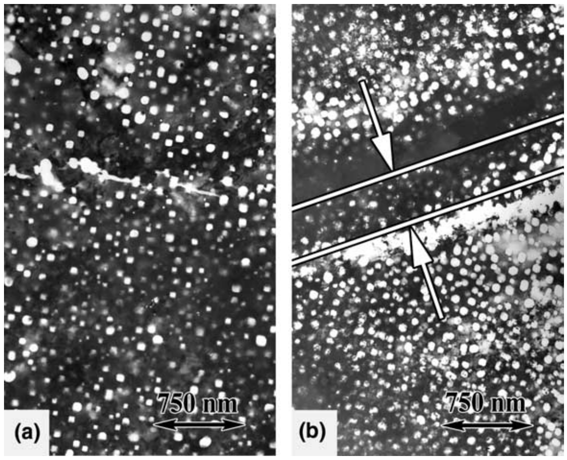

Fig. 3. TEM microstructures of 18Cr–10Ni–Ti SS irradiated at 635 °C to 100 dpa (damage rate 10^{-2} dpa/s) illustration fracture modes during room temperature deformation: (a) matrix area and (b) grain boundary denuded zone.

the non-irradiated material the dislocation multiplication and the dislocation substructure nucleation are not observed.

The amount of strain concentrated in the dislocation channels can be estimated by the shear displacement or offset occurring in microstructural features through which the dislocation channels pass. Fig. 3 shows two dislocation channels that pass through a twin.

From measurement of the channel width (~200 Å, and the component of shear displacement (350–550 Å), we can calculate shear strain in the channel that corresponds in average to about ~150–200% slip dislocation per plane within the channel.

The amount of stress localized at a grain boundary by dislocation channeling can be evaluated by using Koehler's model [5]. When $\boldsymbol{n}$ dislocations pile up against a grain boundary, the stress at the grain boundary surface ($\boldsymbol{\sigma}_g$) can be calculated from the applied stress in the glide plane ($\boldsymbol{\sigma}$) to be equal to $\boldsymbol{n\sigma}$. Taking 550 MPa as $\boldsymbol{\sigma}$ from the tensile test at 300 °C [3], and 1, 5–2 as $\boldsymbol{n}$, the value of $\boldsymbol{\sigma}_g$ turns out to be 900–1000 MPa. This is far greater than the 640–650 MPa value for the grain boundary strength of steel [6].

3.2.3. Deformation in the swelling regime ($T_{irr} = 635$ °C, 10^{-2} dpa/s, 100 dpa)

The defected structure of high-dose deformed specimens (100 dpa, 635 °C) is characterized by a high value of porosity ($\geqslant$ 20%) and by the contribution of porosity to the process of steel fracture (the radiation embrittlement).

This contribution may be separated into two components: matrix and the grain boundary. The crack propagation into the grains proceeds due to the localization of gliding along the voids line (under the stresses the growth of the voids is observed) (Fig. 3(a)).

Irradiation also led to changes in the near-boundary regions in the form of defect-denuded zones as illustrated in Fig. 3(b). In the grain boundary areas the failure proceeds not along the grain boundary but on the distances of 0.4–0.5 μm from the boundary due to the presence of the increased void concentration in these areas (compared with the boundary and with the matrix).

Fracture stress ($\boldsymbol{\sigma}_f$) was estimated according to the radiation voids softening model [7]. The ($\boldsymbol{\sigma}_f$) value ($\leqslant$ 300 MPa) is far lower the 700–730 MPa value for the failure stress of unirradiated 18Cr–10Ni–Ti SS.

Acknowledgements

This work was performed under financial support of Science and Technical Center of Ukraine (Project 2149). Special acknowledgments are due to V.I. Savchenko who has performed samples mechanical testing.

References

[1] A.F. Roweliffe, S.J. Zinkle, J.E. Stubbius, Alexander, J. Nucl. Mater. 258–263 (1998) 183.
[2] E.V. van Osch, M.I. de Vries, M.G. Horsten, J. Nucl. Mater. 258–263 (1998) 301.
[3] I.M. Neklyudov, V.N. Voyevodin, A.A. Parkhomenko, L.S. Ozhigov. In: Abstracts 10th International Conference on

Fusion Reactor Materials (14–19.10.2001.) Baden–Baden, Germany, p.174.

[4] S.M. Bruemmer, J.I. Cole, R.D. Carter, G.S. Was, Mat. Res. Soc. Symp. Proc. 439 (1997) 437.

[5] J.S. Koehler, Phys. Rev. 85 (1952) 480.

[6] A.A. Parkhomenko, Problems of Atomic Science and Technology, Se Radiation Damage Physics and Radiation Material Science, vol. 72, 1998, p. 54 (in Russian).

[7] A.V. Kozlov, I.A. Portnykh, S.V. Bryushkova, E.A. Kinev, Fizika Metallov i Metallovedenie 95 (2003) 87 (in Russian).